

Determination of Irreducible Water Saturation Using Different Experimental Methods

Fan Zheng^{1,2,3}

¹School of Earth Science and Engineering, Xi'an Shiyou University, Xi'an, China

²Shaanxi Key Laboratory of Petroleum Accumulation Geology, Xi'an Shiyou University, Xi'an, China

³No. 4 Gas Production Plant, PetroChina Changqing Oilfield Company, Xi'an, China

Email: 897302339@qq.com

How to cite this paper: Zheng, F. (2025). Determination of Irreducible Water Saturation Using Different Experimental Methods. *Journal of Geoscience and Environment Protection*, 13, 39-50.
<https://doi.org/10.4236/gep.2025.135003>

Received: April 21, 2025

Accepted: May 11, 2025

Published: May 14, 2025

Copyright © 2025 by author(s) and

Scientific Research Publishing Inc.

This work is licensed under the Creative

Commons Attribution International

License (CC BY 4.0).

<http://creativecommons.org/licenses/by/4.0/>



Open Access

Abstract

Bound water saturation is a key parameter in reservoir evaluation and plays a significant guiding role in the formulation of oilfield development strategies. This study focuses on the G region and systematically analyzes the reservoir's microscopic pore-throat characteristics, original oil saturation, and bound water saturation using integrated experimental methods. Specifically, high-pressure mercury intrusion (MICP) was employed to characterize the microstructure of pore-throats, while bound water saturation was determined using a combination of relative permeability tests, nuclear magnetic resonance (NMR) technology, and MICP. The results show that: 1) The main types of reservoir space in the study area are primary and secondary pores. Primary pores are predominantly residual intergranular pores, with chlorite films and authigenic clay minerals developed along pore edges. 2) When using the T_2 spectral area ratio method in NMR logging to determine bound water saturation, the difficulty in accurately defining the T_2 cutoff value (T_2 cutoff) leads to imprecise results. Furthermore, the calculated saturation does not account for bound water present in movable water pores, resulting in systematically underestimated values. 3) The MICP method offers advantages such as fast testing speed, wide measurement range, and minimal requirements on sample size and shape. However, it also presents a discrepancy in wetting characteristics compared to actual oil-water systems. 4) Given the tight nature of the reservoir in the study area, treating the critical water saturation point as a proxy for bound water saturation may introduce certain errors. Thus, the applicability of this approach is relatively limited compared to the other two methods and should be applied with caution.

Keywords

Bound Water Saturation, Relative Permeability, High-Pressure Mercury

1. Introduction

NMR logging methods for evaluating bound water saturation primarily include the thin-film and bimodal models. Various approaches, such as gradient cutoff and T_2 spectral coefficient methods, have been applied to determine the proportion of bound water in pores of different sizes (Chen et al., 2016; Zhang et al., 2018). For the bimodal model, the fixed T_2 cutoff value approach is predominantly adopted, where core NMR experiments and core calibration methods are the two main techniques to determine T_2 cutoff values (T_c) (Wei et al., 2015; Liu et al., 2017). Besides the commonly used fixed T_2 cutoff method, an improved variable T_2 cutoff method has also been proposed (Wang et al., 2019). Based on this method, Su et al. proposed a permeability Coates model using variable T_2 cutoff values and validated its accuracy through core analysis experiments (Su et al., 2021). This approach not only enhances the precision of NMR-derived bound water saturation but also determines regional empirical coefficients (C , m , n) required by the Coates model (Coates et al., 1999).

In laboratory practice, bound water saturation is often measured by mercury intrusion porosimetry (MIP), relative permeability, and semi-permeability methods (Zhang et al., 2014; Yao et al., 2020). Additionally, numerous scholars evaluated bound water saturation through experimental methods. Sui et al. interpolated the capillary pressures obtained from mercury intrusion experiments, calculated average bound water saturation values based on interpolated data, and developed a fitting formula correlating these values with porosity-permeability data (Sui et al., 2018). Xu and Zhang combined rock electrical measurements with mercury intrusion porosimetry to study bound water saturation in tight reservoirs with low porosity and permeability, observing higher saturation from electrical experiments compared to mercury intrusion. By integrating these methods, they proposed a more accurate calculation model (Xu & Zhang, 2019). Pan utilized differences in dielectric properties between bound water and free water, quantifying rock dielectric properties through capacitance measurements of geometrically identical samples, thereby quantitatively evaluating bound water saturation (Pan et al., 2015).

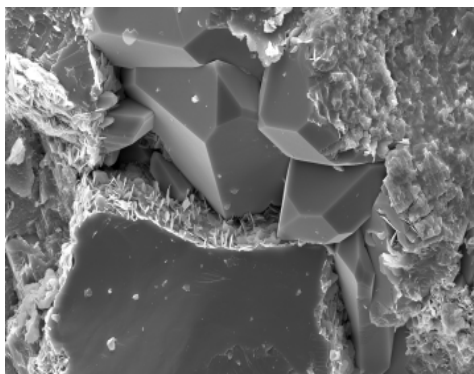
This paper conducts relevant research on the Chang 7 interval in area G, determining its bound water saturation.

2. Microscopic Pore-Throat Characteristics

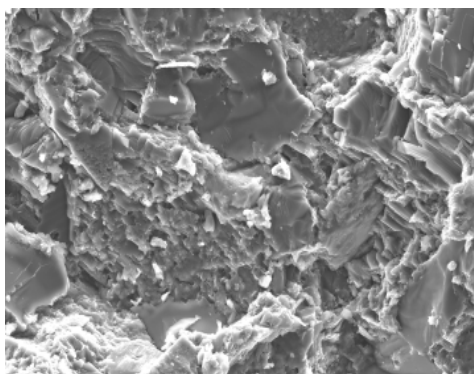
2.1. Pore Types

The tight sandstone reservoirs of the Chang 7 Member in the G area are primarily composed of primary and secondary pores (Figure 1). The primary pores are mainly residual intergranular pores, typically irregular in shape and independently

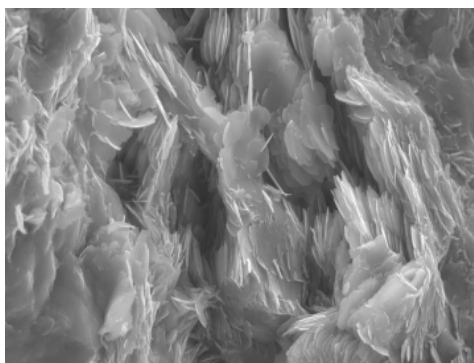
distributed. At the margins of these pores, chlorite coatings and authigenic clay minerals can often be observed.



(a) Quartz cement filling in intergranular pore-throat



(b) Authigenic chlorite clay filling in residual pores



(c) Minor quartz overgrowth in intergranular pore throats

Figure 1. Scanning electron microscope (SEM) images of reservoir characteristics in the study area.

2.2. Analysis of Microscopic Pore-Throat Characteristics Based on High-Pressure Mercury Injection (HPMI) Method

Through high-pressure mercury intrusion analysis of the samples, three key parameters—pore-throat size, sorting, and connectivity—were statistically evaluated to further investigate the pore structure characteristics of the target reservoir layer. As shown in **Table 1**:

Table 1. Pore structure parameters of the reservoir.

| Mercury Injection Parameters | Median Radius (μm) | Median Pressure (MPa) | Displacement Pressure (MPa) | Sorting Coefficient | Skewness | Coefficient of Variation | Maximum Mercury Saturation (%) | Mercury Withdrawal Efficiency (%) |
|------------------------------|---------------------------------|-----------------------|-----------------------------|---------------------|----------|--------------------------|--------------------------------|-----------------------------------|
| Average | 0.07 | 13.51 | 3.04 | 1.26 | -0.81 | 0.09 | 75.78 | 26.35 |
| Maximum | 0.13 | 46.44 | 10.71 | 1.73 | 0.31 | 0.14 | 93.37 | 42.39 |
| Minimum | 0.00 | 0.00 | 1.03 | 0.79 | -5.92 | 0.05 | 35.25 | 20.61 |
| Median | 0.11 | 7.11 | 1.19 | 1.48 | -0.07 | 0.11 | 83.79 | 21.21 |

1) Pore-Throat Size Parameters

This category includes median radius, median pressure, and displacement pressure. The median radius reflects the average size of the pore throats; a smaller value indicates poorer reservoir quality. The median pressure is indicative of oil productivity within oil-water zones, where higher values suggest a tighter reservoir. Displacement pressure represents the maximum radius of the connecting paths between pores and throats, thereby reflecting the volume and distribution of throats. In the study area, the median radius ranges from 0 to 0.13 μm , with an average of 0.07 μm and a median of 0.10 μm ; the median pressure ranges from 0 to 46.44 MPa, averaging 13.51 MPa with a median of 7.11 MPa; displacement pressure ranges from 1.02 to 10.71 MPa, with an average of 3.04 MPa and a median of 1.19 MPa. The relatively large median radius suggests better physical properties, while the high median pressure indicates tight reservoir characteristics.

2) Pore-Throat Sorting Parameters

These include the sorting coefficient (S_p), skewness (S_{kp}), and coefficient of variation. The S_p value reflects the uniformity of pore-throat distribution, with values approaching zero indicating better sorting and more uniform distribution. S_{kp} is used to assess asymmetry in the distribution: $S_{kp} > 0$ indicates positive (coarse) skewness, while $S_{kp} < 0$ indicates negative (fine) skewness. In this area, the sorting coefficient ranges from 0.79 to 1.73, with an average of 1.26 and a median of 1.47; skewness ranges from -5.92 to 0.30, averaging -0.80 with a median of -0.07; the coefficient of variation ranges from 0.05 to 0.14, with an average of 0.07 and a median of 0.11. These results demonstrate good sorting with predominantly fine skewness.

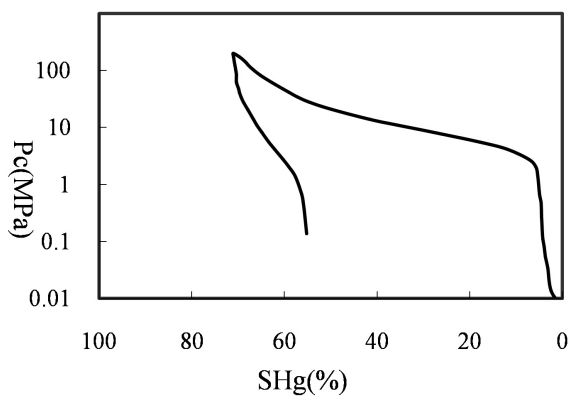
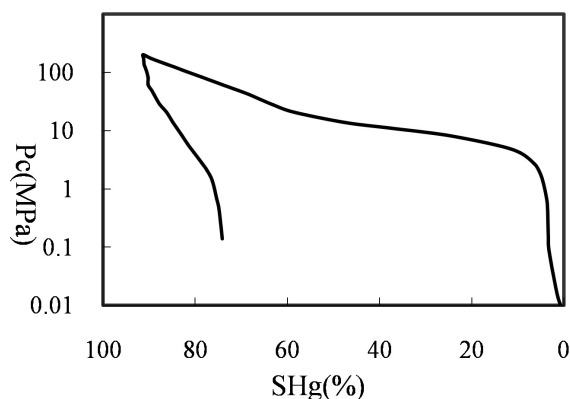
3) Pore-Throat Connectivity Parameters

These parameters include maximum mercury saturation and mercury withdrawal efficiency. Mercury withdrawal efficiency reflects the volume proportion of throat connectivity-higher efficiency suggests better pore-throat connectivity. In this area, the maximum mercury saturation ranges from 35.25% to 93.37%, with an average of 75.78% and a median of 83.79%; mercury withdrawal efficiency ranges from 20.60% to 42.39%, averaging 26.35% with a median of 21.20%. The generally high values for both parameters indicate good pore-throat connectivity in the studied reservoir.

A total of 17 samples from the study area were subjected to high-pressure mercury intrusion experiments, which revealed that the overall physical properties of

the samples are relatively poor. Based on the characteristics of the mercury intrusion/ejection curves and pore-throat distribution (Figure 2), three primary types of capillary pressure curves were identified: concave-shaped, linear-shaped, and a combination of concave and linear forms. Samples from Well D22 predominantly exhibit a combined concave-linear curve, with maximum mercury saturation generally exceeding 80% and the lowest displacement pressures, indicating a more favorable pore-throat distribution and larger storage space. Despite this, the mercury intrusion volume and displacement pressures for D22 samples suggest that while the storage capacity is high, the reservoir remains relatively tight. The pore-throat distributions of the remaining samples fall between these characteristic types and represent the dominant pore structure pattern in the study area. The median pore throat radius ranges from 0 to 0.13 μm , with an average of 0.07 μm and a median of 0.10 μm , indicating that the reservoir is primarily composed of small pore throats.

High-pressure mercury intrusion (HPMI) is a key technique for evaluating pore-throat structures in reservoirs, providing data such as pore radius distribution, capillary pressure curves, and effective porosity. During the HPMI process, mercury gradually invades the rock pores as external pressure increases. The maximum mercury saturation (SHg_{max}) observed at the highest applied pressure represents the proportion of pore volume accessible to mercury, thus indirectly reflecting the development degree of relatively open pore throats in the reservoir.



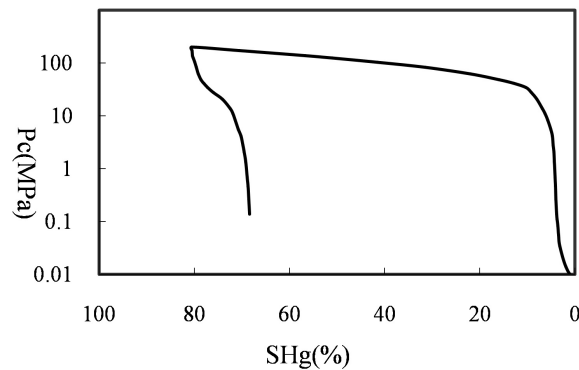


Figure 2. Capillary pressure characteristics from mercury injection tests.

Since irreducible water mainly exists in micropores or poorly connected throats with high capillary pressure, which are typically inaccessible to mercury during injection, it is feasible to estimate irreducible water saturation (S_{wb}) using the following simplified relationship:

$$S_{wb} \approx 1 - SHg_{\max}$$

This estimation is based on several assumptions: 1) the core sample is completely dried before testing; 2) the applied pressure during HPMI is sufficiently high to penetrate most movable pores; and 3) the volume not invaded by mercury is mainly occupied by bound water. In tight sandstone reservoirs, this method offers practical value for rapid estimation of S_{wb} , especially in scenarios where conventional logging fails to effectively identify bound fluids.

However, this method is still subject to uncertainties in practice. Factors such as complex wettability, organic matter presence, or insufficient maximum pressure during testing may lead to deviations in S_{wb} estimation. Therefore, it is recommended to combine HPMI results with nuclear magnetic resonance (NMR) or centrifuge-based methods to improve the accuracy of irreducible water saturation evaluation.

3. Determination of Irreducible Water Saturation Using Integrated Methods

Irreducible water saturation is one of the key parameters for characterizing reservoir properties. It plays a crucial role in hydrocarbon reservoir evaluation, reserve estimation, and productivity forecasting. With the ongoing progress of petroleum exploration and development, reservoirs with low porosity and low permeability have become increasingly prominent in terms of hydrocarbon reserves. In such reservoirs, irreducible water saturation serves as a critical threshold for two-phase flow of oil and water. Therefore, investigating the irreducible water saturation in low-porosity, low-permeability reservoirs holds significant practical relevance.

In this study, several practical and commonly used methods were employed to investigate the irreducible water saturation characteristics of the target area, based on its specific geological conditions.

3.1. Determination of Irreducible Water Saturation Using NMR Method

Nuclear Magnetic Resonance (NMR) is a widely adopted modern technique capable of accurately analyzing rock samples of various shapes and sizes. It can provide detailed information about the fluids present in rock samples and offers distinctive advantages in determining irreducible water saturation. This study introduces an NMR-based method for evaluating irreducible water saturation in core samples. The underlying principle is that irreducible water is subjected to strong surface forces on the solid matrix, resulting in shorter relaxation times, while movable water experiences weaker surface interactions and thus exhibits longer relaxation times.

Based on prior research, this experiment utilizes the significant difference in relaxation times between movable and irreducible water. By determining a T_2 cutoff value corresponding to the movable fluid threshold in a centrifugation model, it becomes possible to distinguish between movable and irreducible water and thereby obtain the irreducible water saturation.

The NMR-based experimental procedure is as follows: First, fully saturated core samples are scanned using NMR to obtain the transverse relaxation time distribution (saturated T_2 spectrum). The saturated cores are then subjected to centrifugation to remove the movable water, leaving only irreducible water. Subsequent NMR measurements are performed on the centrifuged cores to obtain the post-centrifugation T_2 spectrum. The T_2 cutoff value is determined by comparing the saturated and post-centrifugation T_2 distributions. The ratio of the cumulative signal area below the T_2 cutoff to the total T_2 signal area yields the irreducible water saturation as measured by NMR.

Given the absence of free water under a centrifugal force equivalent to a $0.1 \mu\text{m}$ pore throat radius, several representative tight sandstone samples were selected and tested using five different cutoff thresholds for movable fluids ($1 \mu\text{m}$, $0.5 \mu\text{m}$, $0.25 \mu\text{m}$, $0.1 \mu\text{m}$, and $0.075 \mu\text{m}$). NMR tests were conducted under these thresholds (with $T_w = 6 \text{ s}$ and echo spacing $TE = 0.2 \text{ ms}$). Results indicated that $0.075 \mu\text{m}$ is the optimal cutoff threshold for movable fluid in tight sandstone, as it yields irreducible water saturation values that most closely approximate actual conditions in the samples.

The irreducible water saturation results obtained from NMR testing of selected samples from the study area are presented in **Table 2**.

Table 2. Irreducible water saturation of samples measured under a movable fluid threshold of $0.075 \mu\text{m}$.

| Sample No. | Irreducible water Saturation (%) |
|------------|----------------------------------|
| D4 | 92.78 |
| D5 | 83.47 |
| Z1 | 51.41 |

Continued

| | |
|----|-------|
| Z2 | 54.77 |
| Z3 | 56.39 |
| 2 | 60.54 |
| 4 | 63.50 |
| 5 | 53.24 |
| 6 | 65.52 |
| 24 | 45.52 |
| 25 | 65.60 |
| 42 | 84.35 |
| 50 | 87.76 |
| 90 | 84.19 |
| 96 | 91.51 |

3.2. Determination of Irreducible Water Saturation by Mercury Injection Capillary Pressure (MICP) Method

The constant-pressure mercury injection method, which uses mercury as the displacing medium, is a conventional technique for measuring capillary pressure curves. In this context, irreducible water saturation is typically determined under the condition that the applied centrifugal force generates a capillary pressure equivalent to 0.690 MPa (converted to a gas-water system). At this point, the remaining water within the rock sample is considered irreducible.

Therefore, in tight sandstone samples, only when the measured capillary pressure reaches a certain threshold can the remaining water in the sample be regarded as irreducible water. When the mercury saturation reaches 50%, the corresponding capillary pressure is known as the median pressure, and the associated pore throat radius is the median radius. Since the median pressure derived from mercury injection provides higher measurement precision and better reflects pore throat characteristics, this parameter is often used to analyze the relationship between median pressure and porosity in core samples.

By examining this relationship, the point of maximum curvature in the curve is determined using principles from analytical geometry. This point indicates where the median pressure-porosity curve deviates most from linearity, showing the greatest “bend” and thus the highest sensitivity to changes in porosity. This inflection point represents the lower porosity limit of the reservoir’s effective thickness. Below this threshold, the formation cannot produce mobile fluids, and the water present exists solely as irreducible water. The median capillary pressure corresponding to this point is thus referred to as the characteristic pressure in MICP analysis, under which all remaining water is considered irreducible.

In this study, a total of 17 core samples from the study area were analyzed using the MICP method. The resulting capillary pressure curves are shown in **Figure 3**, and the irreducible water saturation values derived from the 17 samples are sum-

marized in **Table 3**.

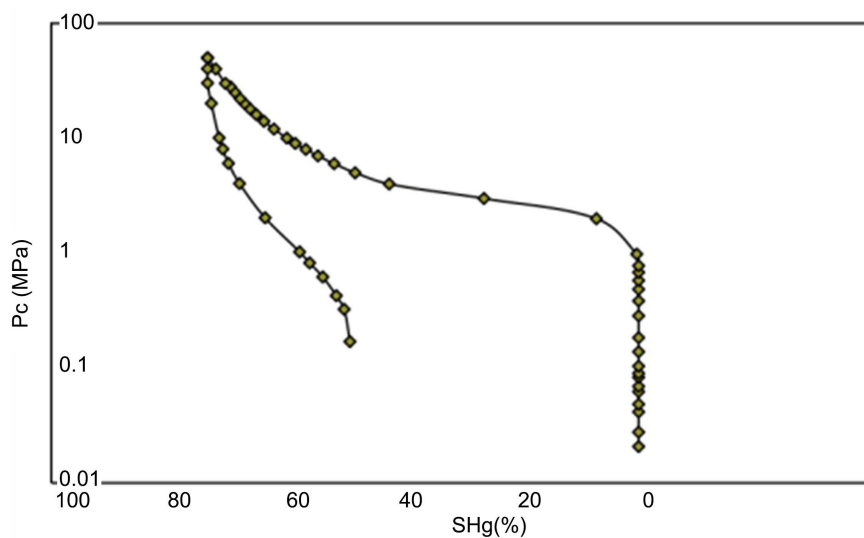


Figure 3. Capillary pressure curves.

Table 3. Bound water saturation determined by mercury injection method.

| Bound Water Saturation (%) | Porosity (%) | Permeability (mD) | Median Pressure (MPa) | Median Pore Radius (μm) | Displacement Pressure (MPa) |
|----------------------------|--------------|-------------------|-----------------------|--------------------------------------|-----------------------------|
| 27.24 | 8.8 | 0.07 | 5.56 | 0.13 | 1.02 |
| 21.56 | 8.0 | 0.08 | 17.94 | 0.04 | 3.6 |
| 24.21 | 5.2 | 0.04 | 15.72 | 0.04 | 4.29 |
| 22.18 | 10.7 | 0.03 | 7.94 | 0.09 | 1.71 |
| 8.74 | 5.9 | 0.02 | 6.96 | 0.1 | 2.18 |
| 18.41 | 5.4 | 0.05 | 7.45 | 0.09 | 1.67 |
| 64.75 | 7.6 | 0.02 | 0.0 | 0.0 | 10.71 |
| 14.55 | 8.7 | 0.49 | 6.91 | 0.1 | 1.18 |
| 16.21 | 9.3 | 0.06 | 7.11 | 0.1 | 1.19 |
| 16.05 | 8.7 | 0.02 | 20.02 | 0.03 | 3.9 |
| 6.63 | 9.8 | 0.08 | 6.84 | 0.1 | 2.16 |
| 20.47 | 8.2 | 0.11 | 7.71 | 0.09 | 1.69 |
| 20.88 | 9.2 | 0.22 | 7.77 | 0.09 | 1.69 |
| 41.31 | 8.2 | 0.01 | 42.47 | 0.01 | 3.43 |
| 18.41 | 6.1 | 0.05 | 7.45 | 0.09 | 1.67 |
| 46.6 | 5.9 | 0.1 | 46.44 | 0.01 | 5.3 |

3.3. Determination of Irreducible Water Saturation Using Relative Permeability Method

The relative permeability curve is a comprehensive reflection of various factors

affecting fluid flow within rock pore channels. It primarily depends on the pore structure of the rock, surface wettability, fluid distribution, saturation sequence, and capillary forces.

In this experiment, 17 core samples were collected from the study area. The water saturation of each sample was measured, and oil-water relative permeability curves were plotted (see **Figure 4**). According to the relative permeability curves, when the relative permeability of oil (K_{ro}) is zero and the relative permeability of water (K_{rw}) is one, the corresponding water saturation at that point on the K_{ro} curve can be considered the irreducible water saturation. Based on this principle, the irreducible water saturation values for the 17 samples were statistically summarized, as shown in **Table 4**.

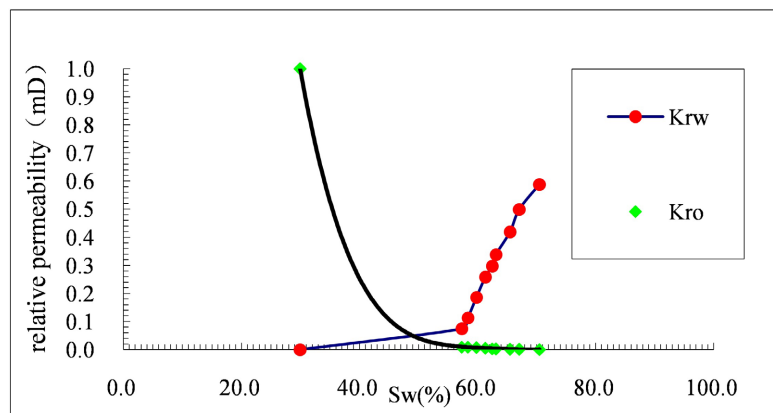


Figure 4. Oil-Water relative permeability curves.

Table 4. Statistical results of irreducible water saturation determined by relative permeability method.

| Sample No. | Irreducible Water Saturation (%) | K_{rw} | K_{ro} |
|------------|----------------------------------|----------|----------|
| 3 | 29.9 | 0.000 | 1.000 |
| 12 | 28.0 | 0.000 | 1.000 |
| 22 | 30 | 0.000 | 1.000 |
| 70 | 24.6 | 0.000 | 1.000 |
| 79 | 25 | 0.000 | 1.000 |
| 86 | 29.5 | 0.000 | 1.000 |
| 95 | 25.1 | 0.000 | 1.000 |
| 112 | 30.7 | 0.000 | 1.000 |
| 133 | 27.0 | 0.000 | 1.000 |
| 147 | 21.9 | 0.000 | 1.000 |
| 158 | 24.1 | 0.000 | 1.000 |
| 167 | 31.2 | 0.000 | 1.000 |
| 180 | 30.3 | 0.000 | 1.000 |
| 189 | 32.8 | 0.000 | 1.000 |

3.4. Advantages of Three Common Methods for Determining Irreducible Water Saturation

In practical reservoir evaluation, High-Pressure Mercury Intrusion (HPMI), Relative Permeability Method, and Nuclear Magnetic Resonance (NMR) are three widely used techniques for determining irreducible water saturation (S_{wb}), each with its own strengths and applicability.

1) High-Pressure Mercury Intrusion (HPMI)

This method quantitatively characterizes pore-throat structures and provides data such as pore size distribution and sealing pore ratio. Irreducible water saturation can be estimated from the maximum mercury saturation, making it suitable for tight and low-permeability reservoirs. It is a mature technique with good repeatability, ideal for multi-well comparative analysis.

2) Relative Permeability Method

Based on oil-water two-phase flow experiments, the obtained S_{wr} has clear physical meaning and reflects the reservoir's real flow behavior. It is closely related to production performance and can be used to calculate movable oil saturation. It also distinguishes reservoir wettability differences.

3) Nuclear Magnetic Resonance (NMR)

NMR offers non-destructive and rapid testing. It uses T_2 spectrum distribution and cutoff values to differentiate movable from bound fluids, which is suitable for complex pore systems like tight sandstones and shales. The results can directly support NMR log interpretation, enhancing field applicability.

4. Conclusion

1) When calculating the irreducible water saturation in the study area using the T_2 cutoff value derived from NMR logging T_2 spectrum and applying the area ratio method, it is difficult to accurately determine the T_2 cutoff value. Moreover, this method excludes the portion of irreducible water residing within the movable water pores, resulting in an overall underestimation of the irreducible water saturation.

2) The mercury intrusion method for measuring irreducible water saturation demonstrates several advantages: fast measurement speed, wide applicable range, and no stringent requirements on the shape or size of the rock sample. However, the method's inherent inconsistency with the actual oil-water wetting characteristics may affect accuracy.

3) Given that the reservoirs in the study area are of low porosity and low permeability (tight reservoirs), the water saturation value is used at the critical point as the irreducible water saturation introduces error. Therefore, this method is less applicable compared to the other two techniques.

Acknowledgements

Thanks to the school and colleagues for their help, as well as the strong support for me.

Conflicts of Interest

The author declares no conflicts of interest regarding the publication of this paper.

References

- Chen, Y. Q., Zhang, J. C., & Chen, Q. (2016). Advances in Evaluating Reservoir Bound Water Saturation Using NMR Logging. *Oil Geophysical Prospecting*, *51*, 582-588.
- Coates, G. R., Xiao, L. Z., & Prammer, M. G. (1999). *NMR Logging Principles and Applications* (pp. 189-207). Halliburton Energy Services.
- Liu, W., Zhou, C. C., & Chen, Q. Y. (2017). Application of Core Calibration for Determining T_2 Cutoff Values in NMR Logging. *Oil & Gas Geology*, *38*, 362-370.
- Pan, B. Z., Sun, Q. H., & Liu, S. (2015). Experimental Determination of Bound Water Saturation Using Dielectric Constant Measurements. *Acta Petrolei Sinica*, *36*, 563-570.
- Su, J. L., Yang, W. G., Wang, Z. Y. et al. (2021). A Permeability Coates Model Based on Variable T_2 Cutoff Values and Its Validation via Core Analysis Experiments. *Natural Gas Geoscience*, *32*, 1120-1130.
- Sui, X. J., Li, Y. P., & Wang, H. (2018). Evaluation of Bound Water Saturation in Tight Sandstone Based on Mercury Intrusion Experiments. *Petroleum Geology & Engineering*, *32*, 89-92.
- Wang, S. C., Liu, H. W., & Zhang, W. Z. (2019). Determination of Bound Water Saturation Using Variable T_2 Cutoff Values in NMR Logging. *Chinese Journal of Geophysics*, *62*, 2715-2723.
- Wei, Z., Li, L., & Liu, J. (2015). Methodology for Determining T_2 Cutoff Values via Core NMR Experiments. *Petroleum Geology & Experiment*, *37*, 502-506.
- Xu, P., & Zhang, C. G. (2019). Determining Bound Water Saturation in Tight Sandstone Reservoirs via Combined Rock Electrical and Mercury Intrusion Methods. *Petroleum Exploration and Development*, *46*, 1155-1162.
- Yao, H., Liu, R. B., & Li, M. X. (2020). Determination of Bound Water Saturation in Low-Permeability Sandstone Reservoirs by Relative Permeability Method. *Lithologic Reservoirs*, *32*, 85-91.
- Zhang, W. W., Huang, J. S., & Chen, G. (2014). Applicability of Mercury Intrusion Method for Determining Bound Water Saturation in Low-Permeability Reservoirs. *Petroleum Geophysical Exploration*, *53*, 451-458.
- Zhang, X. H., Yang, Z. Z., & Liu, J. (2018). Determination of Bound Water Saturation by NMR Logging Gradient Cutoff Method. *Well Logging Technology*, *42*, 60-64.